Nano-Structures & Nano-Objects 36 (2023) 101069

Contents lists available at ScienceDirect

Nano-Structures & Nano-Objects

journal homepage: www.elsevier.com/locate/nanoso

Control of fungal deterioration of ceramic materials by green nanoadditives-based coatings

Erasmo Gámez-Espinosa [a,*], Cecilia Deyá [a,b], Marta Cabello [c,d], Natalia Bellotti [a,d,**]

[a] Centro de Investigación y Desarrollo en Tecnología de Pinturas y Recubrimientos (CONICET-CICBA-Ing.-UNLP), Buenos Aires, Argentina
[b] Facultad de Ingeniería, Universidad Nacional de La Plata, Buenos Aires, Argentina
[c] Instituto de Botánica "Carlos Spegazzini"(CICPBA-UNLP), Buenos Aires, Argentina
[d] Facultad de Ciencias Naturales y Museo, Universidad Nacional de La Plata, Buenos Aires, Argentina

ARTICLE INFO

Keywords:
Nanomaterials
Protective coatings
Fungal deterioration

ABSTRACT

Biodeterioration of building materials causes financial losses as restoration and conservation processes need to be carried out. Filamentous fungi invade the surface of ceramic materials causing fungal deterioration, in these cases, coatings with antimicrobial additives are used to control this phenomenon. This research is aimed to assess the use of sol-gel coating with antifungal nanoparticles to control biodeterioration on ceramic materials. Nanoparticles were obtained by green synthesis using an aqueous solution of tannin from *Schinopsis balansae* and *Caesalpinia spinose*. Moreover, $AgNO_3$ salt, 3-aminopropyltriethoxysilane (AMEO), or 3-mercaptopropyltrimethoxysilane (MTMO) were used as precursors on the sol-gel coatings. Coatings with AMEO and silver nanoparticles showed better antifungal performance to protect ceramic materials, as opposed to those coatings containing MTMO and silver nanoparticles. Therefore, the functionalized sol-gel coatings with antifungal nanoparticles showed their efficiency in the control of fungal deterioration to protect clay bricks.

1. Introduction

The degradation caused by biofouling of microorganisms is one of the main cause of building deterioration, especially of building façades [1,2]. Biodeterioration in building materials (stone, ceramics, cement, concrete, etc.) is a global and costly problem for construction companies [3]. Furthermore, since 2011 it has been claimed that the annual global loss of non-food materials due to fungal attack is 40 million dollars [4], just to mention one group of organisms. However, the cultural and historical value of many buildings is inestimable and therefore cannot simply be expressed in monetary terms. Microorganisms such as bacteria, archaea, protozoa, fungi, and algae play an essential role in all types of the built ecosystems, affecting negatively human health, quality of air and water, properties, and durability of the construction materials in the built environment [5].

Compared to other microorganisms, fungi play an important role in the deterioration of construction materials. Fungi, especially those of the filamentous type, damage the integrity of materials due to their vital activity [6]. Fungal deterioration can be chemical, physical and aesthetic, although the phenomenon should not be analyzed separately, but as a combination of these [7]. Due to their heterotrophic absorptive nutrition, secretion of extracellular enzymes that digest complex molecules and apical hyphal growth, filamentous fungi have a strong ability to grow on surfaces, thus forming biofilms [8,9]. Possibly the survival and proliferation of fungi on materials is related to the ability to form biofilms. In this regard, Harding *et al.*, 2009 [10] proposed a pioneering six step mechanism for the formation of filamentous fungal biofilms based on models for bacteria and yeast. Physical fungal deterioration can occur by expansion of the hyphae throughout the construction material leading to mechanical alterations [11]. That is, as the fungal biofilm grows, shallow and deep cracks are observed that increase the porosity of the materials [7,12]. Furthermore, this increased porosity facilitates the colonization of the materials by other microorganisms and promotes their growth.

On the other hand, Coutinho *et al.*, 2015 [12] and Martino, 2016 [13] state that the first problem of microbial colonization is the unsightly appearance of the material. In fact, the biofilm that develops on the materials is often pigmented. Fungi produce various pigments, such as

* Corresponding author.
** Corresponding author at: Centro de Investigación y Desarrollo en Tecnología de Pinturas y Recubrimientos (CONICET-CICBA-Ing.-UNLP), Buenos Aires, Argentina.
E-mail addresses: e.gamez@cidepint.ing.unlp.edu.ar (E. Gámez-Espinosa), n.bellotti@cidepint.ing.unlp.edu.ar (N. Bellotti).

https://doi.org/10.1016/j.nanoso.2023.101069
Received 16 June 2023; Received in revised form 25 October 2023; Accepted 27 October 2023
2352-507X/© 2023 Elsevier B.V. All rights reserved.

carotenoids, mycosporins and melanins, which protect them from UV irradiation [14]. Melanin mainly provides them with extra mechanical strength and the hyphae can grow better in the fissures. This is not desirable, because the material must remain intact over time. Some authors have pointed to various factors that can play a role in fungal deterioration of building materials [2,15]. Weakening of materials caused by the development of biofilms leads to faster deterioration by accelerating the effects of weathering and advanced biodeterioration leads to loss of structural or thermal insulation, drainage and solar reflectance of materials [16]. Temperature, relative humidity, water content, surface cleaning routines, air renewal and light intensity could lead to the selection of certain microorganisms, interfering with their survival or resistance. Factors such as the type and chemical composition of the material, pH and nutrient availability also need to be taken into account [15].

Ceramic materials like clay bricks are widely used in construction projects as they possess beneficial characteristics such as low cost, high durability, and ease of handling [17,18]. Clay is the primary raw material used in brick production. For brick manufacturing, almost 340 billion tons of clay are used annually [18]. The physical-mechanical characteristics of clay bricks depend on the raw materials' chemical compositions and phase transformation during the firing process. The forming of pores increases clay brick porosity and decreases mechanical properties. However, it improves the thermal conductivity property of the bricks [19,20]. The brick industry represents one of the most traditional manufacturers of construction products, which dominated the market for residential buildings over decades [18]. However, increased requirements for thermal insulation together with building methods based on cementitious materials and cheap external insulation, forced the brick industry to innovate [21]. For example, Lawanwadeekul *et al.* 2023 [19] showed that the strength and porosity of clay brick could be enhanced with the aid of corn cob and waste glass and fired at the low temperature of 900 °C. In addition, Moujoud *et al.* 2023 [20] showed that the use of coconut shells waste powder as pore-forming agent is a valuable way to develop lightweight bricks with promoting thermal insulating character.

Antimicrobial or hygienic coatings containing antifungal additives in their formulation can be used to control fungal growth and thus biofilm development [22,23]. However, in some building materials, paints cannot be applied to control biodeterioration as their original appearance must be maintained for aesthetic reasons, e.g. stone and ceramic materials. Therefore, one of the strategies to obtain antimicrobial coatings is the chemistry related to silicon oxide and the application of the sol-gel process directly on the substrate.

The sol-gel process consists of two stages with very different physicochemical characteristics. The initial stage consists of obtaining a stable colloidal suspension (sol) from a precursor. The subsequent stage results from the destabilization of the sol causing condensation of the monomers/oligomers in suspension, leading to the formation of a polymer (gel). Given the physical and chemical properties of the compounds used, this polymer has the characteristics of coatings with mechanical strength [24,25]. The precursors in the initial stage are typically oxides and alkoxides of metals or silicon. Alkoxysilanes can have different alkyl residues, such as methyl, butyl, etc. Within this group of precursors, organically modified silicates can be found [26]. These are silicon alkoxides in which up to three of the alkoxy residues are replaced by an alkyl residue with a functional group. For example, aminopropyl triethoxysilane, mercaptopropyl trimethoxysilane, phenyl triethoxysilane, and octadecyl trichlorosilane [27,28]. In this way, it is possible to introduce a wide variety of functional groups into the structures of polymeric networks and impart them with the specific chemical characteristics of the introduced residue.

A sol is a colloidal suspension of solid particles in a liquid. The most common method for obtaining a sol from an alkoxide involves hydrolysis followed by the stabilization of monomers in an acidic or alkaline medium. Then, the gelation process begins, consisting of two steps: condensation and polymerization. In the case of SiO_2, particle growth is inevitable, so condensation and polymerization are two parallel processes [29,30]. Subsequent to gelation, controlled gel contraction due to syneresis becomes evident [31]. Syneresis is the contraction of the polymeric network resulting from the expulsion of liquid from the pores. This leads to the condensation of two silanol groups, from two particles that are further apart than the Si-O-Si bonding distance. Only the approach via solvent expulsion from inside the pores can enable this bonding, resulting in increased evaporation and favoring contraction. Syneresis is a critical process when obtaining a gel in the form of a coating [31,32]. Moreover, material aging occurs due to drying through solvent evaporation, along with the syneresis process that releases water for subsequent evaporation [32]. In coatings, the exposed surface area is larger, leading to extensive solvent evaporation, which results in the compaction of the gel (xerogel).

The characteristics of a coating obtained by the sol-gel process are related to the factors that regulate hydrolysis, condensation and polymerization [33]. These factors include pH, temperature, catalysts and reagent concentrations. However, after synthesis, the humidity and ageing time to which the material is exposed also influence the fixation structure and final reactivity [25]. If the surface on which the sol is deposited is hydrophilic, chemically active and the generated gel is thin (~1 μm), the drying after gelation is so fast that it can prevent shrinkage and fracture of the coating. Therefore, this is a compact, homogeneous and adherent coating [34]. One of the most important advantages of sol-gel chemistry is the low viscosity of the sol prior to gelation. For this reason, coatings can be prepared by a wide variety of methods. One aspect reported in the scientific literature regarding sol-gel technology is the methodologies used for surface coating [35,36]. These include vertical immersion, spin-coating, electrophoresis, thermophoresis and surface immobilizations (impregnation, inclusion, chemical and copolymerization).

In the field of sol-gel coating applications, has been regarded as the frequent approach for the realization of silver-based silica nanocomposites, because it has many advantages, such as versatility, feasibility, lower maintenance and operational costs, low-temperature processing, and the ability to control the shape of particles and the size distribution [37]. Within this same context, an efficient microwave-assisted synthesis method was employed to synthesize silica nanoparticles and a nanostructured silica-gentamicin solution in a basic medium. This process involved the use of two silane precursors, tetraethylorthosilicate and octyltriethoxysilane, along with the antibiotic gentamicin sulfate. These sol-gel-derived SiO_2-gentamicin nanohybrids were prepared and characterized for potential antimicrobial applications. Additionally, the versatility of sol-gel coatings extends beyond this, showing promise in medical applications such as enhancing the antimicrobial resistance of orthopedic implants and preventing infections [38,39].

Various antimicrobial compounds such as disinfectants and biocides functionalized in coatings are commonly applied to control the growth of microorganisms [3,40]. Efforts are currently focused on improving the bioactive ingredients used in the formulation, extending their useful life, replacing conventional toxicants, reducing the concentrations used and avoiding their loss in the coating. In this context, the emergence of nanotechnology presents a broad field of study for new functional materials with size-dependent properties [41]. The global nanotechnology market is estimated to reach 131 million dollars by 2026, up from 58 million dollars in 2020 [42]. Nanotechnology applied in the design of antimicrobial surfaces aims to eliminate pathogens in the vicinity of the surface, preventing the formation of biofilms [43].

Nanoparticles (NPs) can be synthesized through physical, chemical, and biological methods. Physical and chemical methods include milling, gamma radiation, the use of microemulsions, electrochemical methods, laser ablation, chemical reduction, photochemical reductions, hydrothermal synthesis, and solvothermal and sonochemical coprecipitation [44]. Physical and chemical methods have low yields and limitations

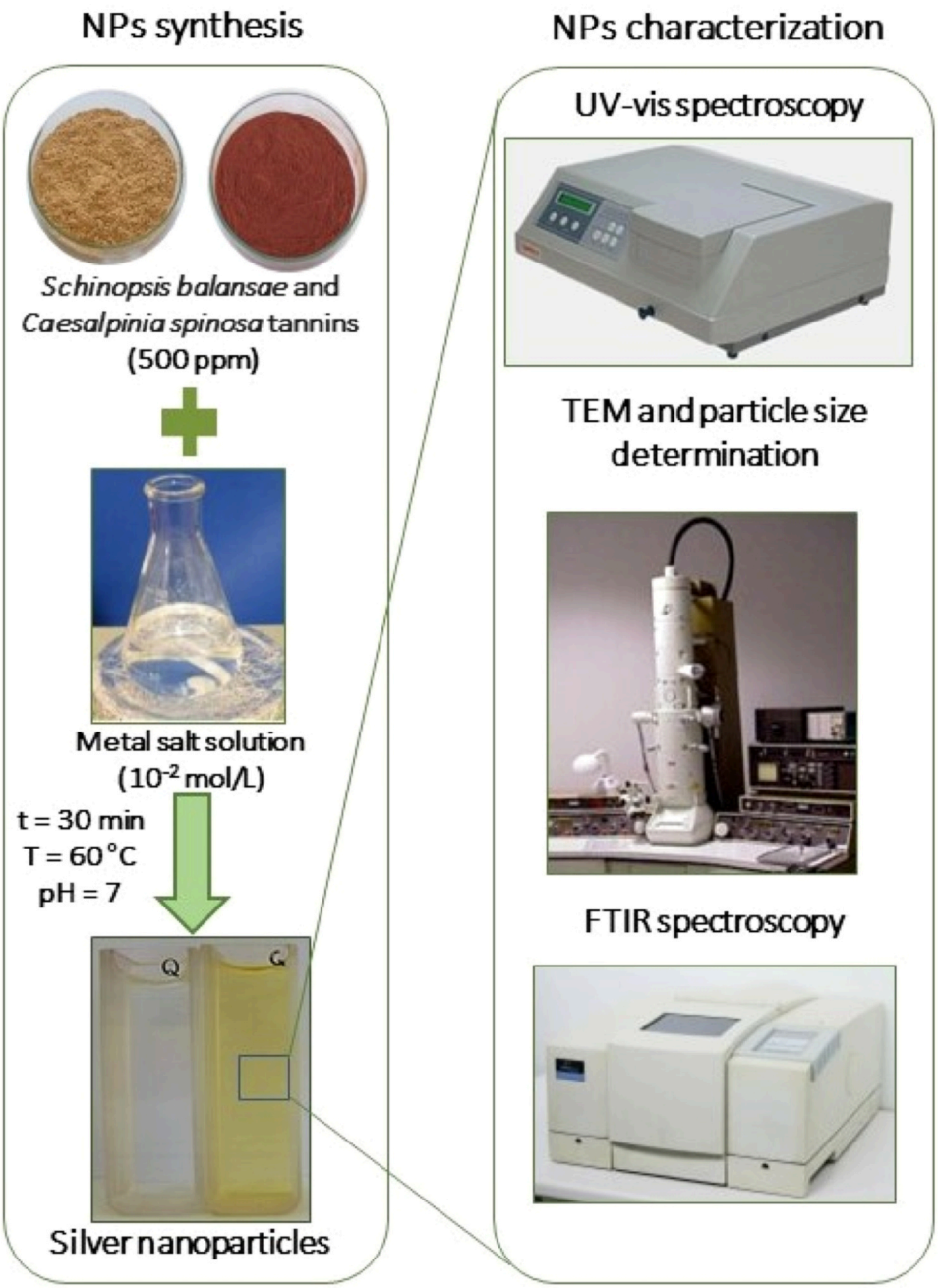

Fig. 1. Schematic diagram of green synthesis and characterization of AgNPs.

such as high functional cost, use of toxic chemicals and high energy supply. Most of these methods often use hazardous chemicals for advanced research of NPs [41,45]. Therefore, the disadvantages of these methods may limit their large-scale production and consequently their applications [46]. To overcome the limitations of physical and chemical methods, cost-effective alternative biological methods using plant extracts (phytosynthesis), fungal cultures (mycosynthesis), bacterial cultures and natural polymers have been used to obtain NPs [46,47]. Obtaining NPs from plant extracts and metal salts solutions has many advantages over traditional methods, such as simplicity of the procedure, absence of contamination and toxicity, possibility of large-scale production and cost-effectiveness [45,48]. These green approaches have sufficient potential to develop well-defined NPs in size and shape for several promising commercial applications [49]. Particularly the use of plants with tannin and high amounts of polyphenols which can function as reducing and stabilizers agents of particles [50]. In this sense, commercial tannins from *Schinopsis balansae* and *Caesalpinia spinosa* were used in the present research work.

Therefore, the aim of this research was to assess the use sol-gel coating with antifungal NPs in the fungal deterioration control of ceramic materials. Silver nanoparticles (AgNPs) were synthesized by green synthesis from two different tannins. Furthermore, they were characterized by various techniques and the antimicrobial activity was evaluated. Then, the particles were functionalized in coatings obtained from different precursors. Finally, the antifungal performance of the coatings on clay bricks against deteriorating fungal strains was evaluated. The novelty of this paper lies in the update of knowledge on sol-gel coating technology through the incorporation of nanomaterials obtained by green synthesis and their application in the prevention of biodeterioration of ceramic materials.

2. Materials and methods

2.1. Biosynthesis and characterization of nanoparticles

AgNPs were synthesized by adding a tannin solution from either *Schinopsis balansae* (TQ) or *Caesalpinia spinosa* (TT) to an aqueous solution of $AgNO_3$. The mixture was stirred for 30 min at 60 °C, and the pH was adjusted to 7 using a 1:1 v/v solution of NH_4OH (99.9%, Anedra, Argentina). The concentration of the TQ or TT solution was 500 ppm and was prepared from the products supplied, with analytical-grade purity, by Unitan (Argentina) and Indunor (Argentina), respectively. The final concentration of the salts in the synthesis system was 10^{-2} mol/L. The resulting nanoparticle suspension was stored in caramel flasks at 4 °C in the refrigerator for 90 days [51].

Subsequently, the AgNPs were characterized using UV-Vis spectroscopy, FTIR spectroscopy, Transmission Electron Microscopy (TEM) observation and particle size determination. The absorbance measurements of UV-Vis spectroscopy were made in a UV SP 2000 spectrophotometer (China) to verify the presence and stability of the NPs in suspension at 1 and 90 days. The NPs were purified through multiple washes using a DLAB D3024R microcentrifuge (China) at 15000 rpm for 20 min at 20 °C. Purified nanoparticle samples were subjected to FTIR spectroscopy using the KBr disk method using a PerkinElmer Spectrum One Spectrometer (United Kingdom) and analyzed using the KnowItAll® Informatics System program, Version: 10.0.19043. TEM analysis was conducted to validate the synthesis of the NPs, examine their morphology and particle size. The equipment used was a JEOL 100 CXII (Japan) at an acceleration voltage of 100 KV. A schematic of the preparation and characterization of the NPs is shown in Fig. 1.

2.2. Antifungal activity of nanoparticles

The antifungal activity of the AgNPs suspensions was determined by macrodilution assay. Malt Extract Agar (MEA) with different concentrations of NPs suspensions (10, 50 and 167 μg/mL) were placed in Petri dishes. The culture medium per liter of distilled water consists of 30 g of malt extract (99.9%, Circe, Argentina), 3 g of mycological peptone (99.9%, Oxoid, United Kingdom) and 15 g of agar (99.9%, Parafarm, Argentina). As a control, NPs-free Petri dishes with MEA (0 μg/mL) were used. Subsequently, the plates were inoculated in the center with 20 μL spore suspension (10^5 spores/mL) and incubated for 7 days at 28 °C. Fungal growth was assessed through the measurement of the colony diameters and the Minimum Inhibitory Concentration (MIC) was determined. The test was carried out in triplicate [23]. The strains selected for this study were *Aspergillus niger* MN371276, *Penicillium commune* MN371392 and *Cladosporium sphaerospermum* MN371394. They were isolated from biodeteriorated façade of the Cathedral of La Plata city in a previous research work [52].

2.3. Characterization of the ceramic material and the formulated coatings

NPs functionalized sol-gel coating was prepared to be applied in the protection of commercial clay bricks (Cerámicos La Plata, Argentina). Untreated bricks were characterized by determining water absorption, relative porosity, apparent specific weight and apparent specific weight in water following the procedure of the IRAM 12510. In addition, Mercury Intrusion Porosimetry (MIP) was determined by a Pascal 440 Thermo Scientific equipment (United States of America).

To the sol-gel coatings, 3-aminopropyl triethoxysilane (AMEO) and 3-mercaptopropyltrimethoxysilane (MTMO) (98.5%, Camsi-X, Argentina) were used as silane precursors and added in a concentration of 2% (v/v). The silane was added under constant stirring to a solution containing: 0.9 mL/mL of ethanol (96°, Purocol, Argentina), 0.06 mL/mL of NPs suspensions and distilled water (DW). The pH was previously adjusted to 4 with HNO_3 (99.9%, Anedra, Argentina). Controls replacing NPs suspension by DW were prepared. After 1 h of hydrolysis, bricks of 4.0 ± 0.4 cm^3 were immersed in the solutions for 90 s and allowed to dry for 14 days at 25 °C [53]. The silane coatings were characterized by contact angles measurements. The contact angle was measured for triplicate by placing a drop of distilled water on the coated brick by a Pasteur pipette, employing a Gaosuo digital microscope (China) [54].

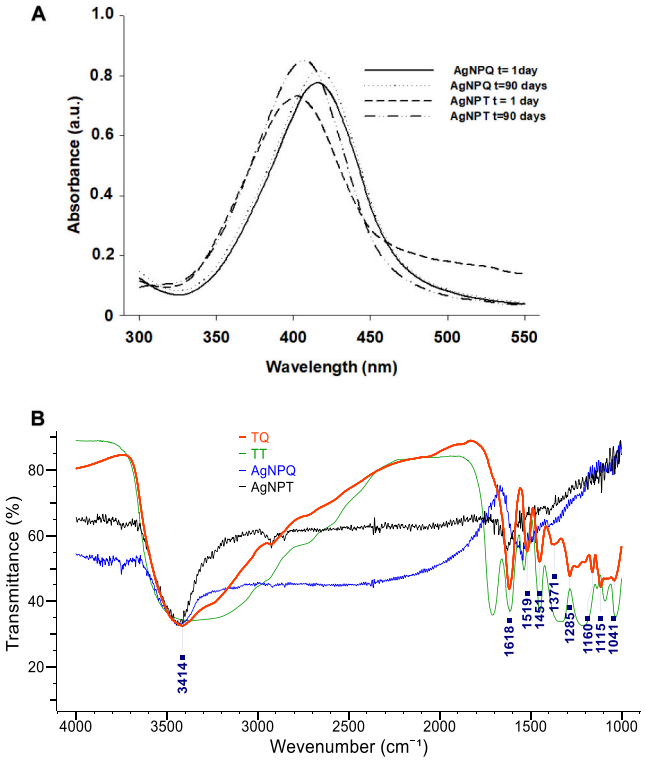

Fig. 2. UV–vis spectra (A) and FTIR spectra (B) of AgNPs synthesized with *S. balansae* and *C. spinosa* tannin.

2.4. Fungal resistance test of coatings

The bricks with the NPs-functionalized coatings were placed in Petri dishes with 10 mL of Minimum Mineral Agar (MMA). The culture medium per liter of distilled water consists of 5 g of NaCl (99.9%, Anedra, Argentina); 3 g of KNO_3 (99.9%, Mallinckrodt, United States of America); 1 g of HK_2PO_4 (99.9%, Anedra, Argentina); 1 g of $(NH_4)H_2PO_4$ (99.9%, Biochem, Argentina); 0.2 g of $MgSO_4$ (99.9%, Anedra, Argentina) and 15 g of agar (99.9%, Parafarm, Argentina). Each one was inoculated with the same volume (50 μL) of a spore solution (10^5 spores/mL). The fungal strains were *A. niger*, *P. commune* and *C. sphaerospermum*. Petri dishes were incubated at 28 °C for 30 days. The fungal growth observed on the samples was reported as a percentage (%) of the covered area, categorized as follows: 0% (no growth), < 10%, 10–30%, 30–60%, and 60–100%. These categories were further classified as 0, 1, 2, 3, and 4, respectively [55].

At the end of the test, the samples were observed by stereo microscopy (Leica S8 APO, Germany) and Scanning Electron Microscopy (SEM) with the Philips FEI Quanta 200 (United States of America). For SEM observation, the samples were prepared following the methodology proposed by Simões *et al.*, 2013 [56]. First, they were immersed in a 2.5% glutaraldehyde solution (25.0%, Sigma-Aldrich, United States of America) in phosphate buffered saline (PBS). In the preparation of PBS, 8 g NaCl (99.9%, Anedra, Argentina), 0.14 g KH_2PO_4 (99.9%, Anedra, Argentina) and 0.9 g K_2HPO_4 (99.9%, Anedra, Argentina) were added per litre of DW. Subsequently, for dehydration, these were embedded in 20%, 50%, 70%, 90% and 100% ethanol solutions (Absolute, Soria,

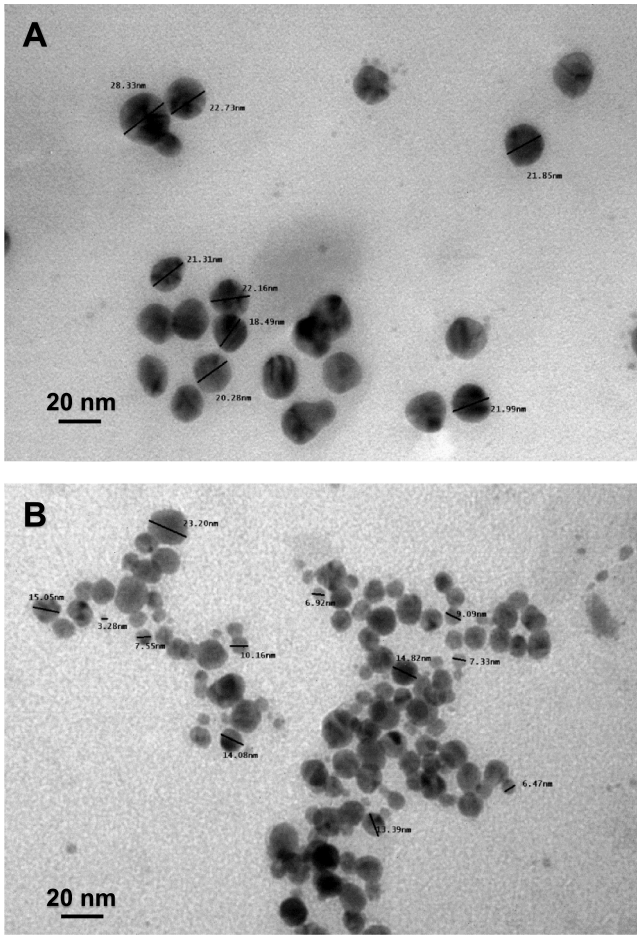

Fig. 3. TEM images (450000x) and size distribution analysis. A: AgNPQ and B: AgNPT.

Argentina) for 30 min in each solution. Finally, the sample was directly covered with gold and the working conditions were under high vacuum (10^{-6} torr).

Table 1
Macrodilution test: minimum inhibitory concentration (μg/mL).

Strain	AgNPQ	AgNPT
A. niger	167	> 167
P. commune	50	50
C. sphaerospermum	≤ 10	≤ 10

3. Result and discussion

3.1. Biosynthesis and characterization of nanoparticles

It is often preferable if the AgNPs were synthesized using non-harmful, environmentally safe methods rather than toxic chemicals. The green synthesizes of AgNPs using various plant extracts add additional properties such as low cost, ability to monitor size or surface morphology and they could have antiviral, antibacterial or antifungal activity [57]. From TQ and TT it was possible to obtain AgNPs, which were labeled as AgNPQ and AgNPT respectively. Fig. 2A shows the UV–vis spectra of the NPs suspensions obtained. Peaks between 400 and 450 nm corresponding to the surface plasmon band of AgNPs can be observed in both cases. The wavelengths position depends mainly on the size, shape and particle size distribution [58]. Spectroscopic measurements of the AgNPs suspensions stability over time were performed. The absorption bands peaks stayed with the same wavelengths, which shows that the NPs suspensions were stable. Both AgNPQ and AgNPT absorption peaks increase intensity after 90 days.

Fig. 2B shows the FTIR spectra of the tannins and NPs, there are well resolved peaks at 3414 and between 1618 and 1000 cm^{-1}. Peaks between 3600 and 3400 cm^{-1} corresponding to the stretching of the O-H group and the peak at 1618 cm^{-1} assigned to carbonyl groups stretching that are present in this kind of polyphenol [50,59]. Nevertheless, peaks between 1500 and 1000 cm^{-1}, due to the stretching of C-C, correspond to phenols [60]. The peaks corresponding to AgNPQ and AgNPT are shifted to lower frequencies by electrical effects due to the release of electrons during the reduction of metal ions and the formation the particles. The presence of these functional groups in the purified AgNPQ and AgNPT may indicate that they are strongly associated with the polyphenol. Then the polyphenols of TQ and TT would reduce Ag^{+} ions to Ag°, acting as a reducing agent and green stabilizer.

TEM analysis explains the size and morphology of the obtained particles. TEM images demonstrated that the synthesized AgNPs were quasi-spherical and dispersed (Fig. 3). The average size of AgNPQ and AgNPT was 22 and 12 nm, respectively. NPs having a different average size possibly because they were obtained from distinct tannins. NPs size is influenced by tannin concentration in the synthesis. According to Restrepo *et al.* [61], UV–vis absorption spectra and TEM images of the AgNPs indicate that higher concentration of tannin may cause increased size and polydispersity of the NPs. Consequently, in the present work a low concentration of tannin (500 ppm) was used to obtain small NPs. Therefore, the composition of the plant extract affects the morphology of the synthesized NPs significantly and because same plant extracts contain same concentrations of biochemical reducing agents, then the source of the tannin can be considered a key factor. In addition, the temperature plays an important role in morphology control. For example, at 60 °C, triangle or polygon shapes are produced and under boiling conditions, quasi-spherical particles are produced as a result of reduction, nucleation, and crystallization of Ag^{+} [62,63].

3.2. Antifungal activity of nanoparticles

Table 1 shows the MIC for macrodilution assay. When *A. niger*, *P. commune* and *C. sphaerospermum* faced AgNPQ, the MIC was 167, 50 and ≤ 10 μg/mL respectively. The same MIC values were recorded when *P. commune* and *C. sphaerospermum* were exposed to AgNPT, however there were differences against *A. niger* (>167 μg/mL). Therefore,

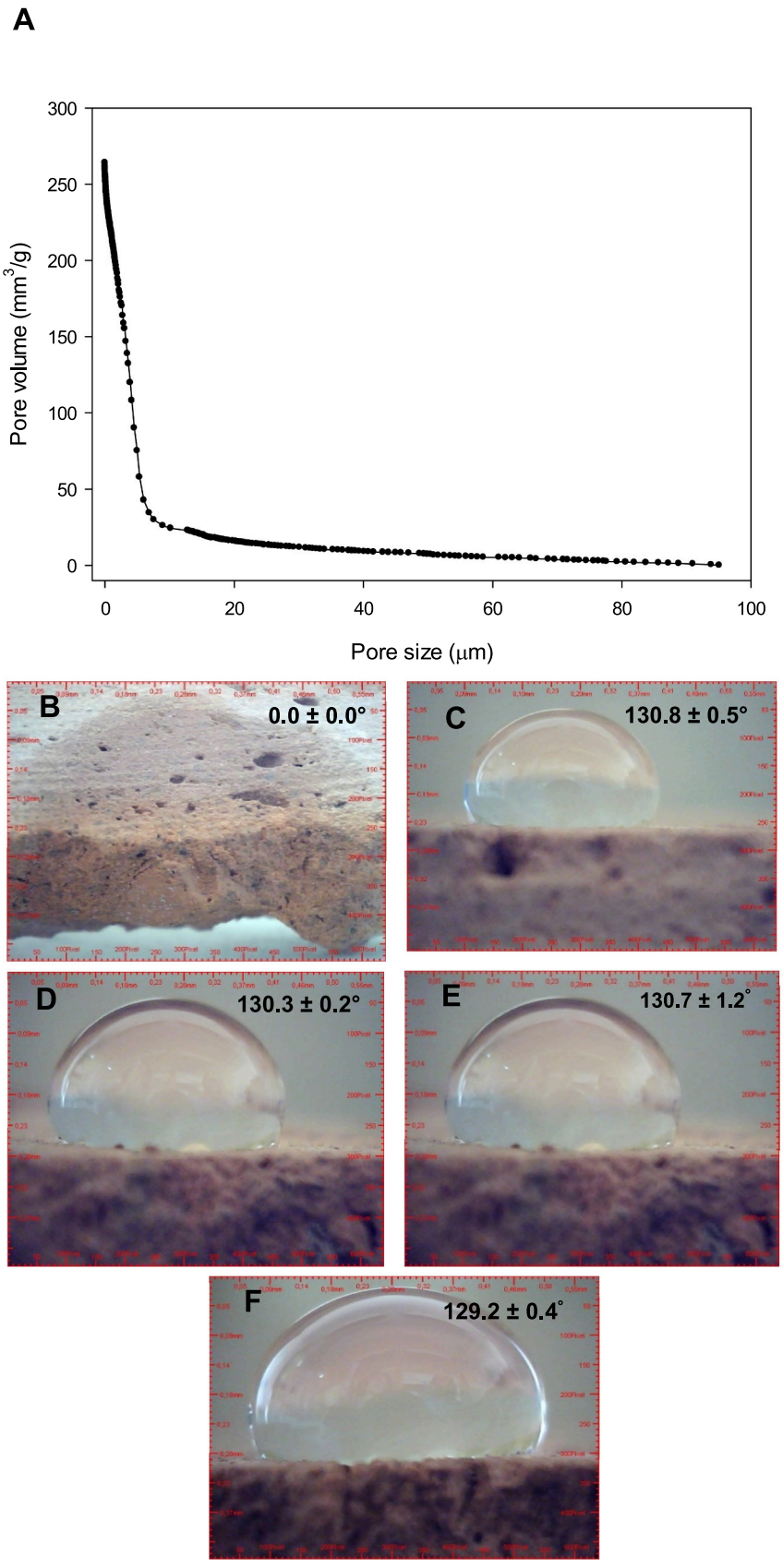

Fig. 4. Porous distribution by MIP of clay brick (A) and Water contact angle on bricks (B-F). B: Without treatment (control); C: AMEO + AgNPQ; D: AMEO + AgNPT; E: MTMO+ AgNPQ and F: MTMO + AgNPT.

Table 2
Fungal growth rating according to the area covered.

Brick treatments	*A. niger*	*P.commune*	*C. sphaerospermum*
Control	4	4	3
AMEO	3	3	3
AMEO+ AgNPQ	0	0	0
AMEO+ AgNPT	0	1	0
MTMO	4	3	2
MTMO+ AgNPQ	2	2	1
MTMO+ AgNPT	2	2	1

Note: 0 (none 0%), 1 (growth in traces < 10%), 2 (light growth 10– 30%), 3 (moderate growth 30–60%) and 4 (heavy growth 60–100%).

AgNPQ has better antifungal activity than AgNPT against the strains selected in the macrodilution assay. Several researchers have reported on the possible mechanism of interaction of AgNPs with fungal strains [64]. It has been reported that AgNPs bind to the cell wall and cell membrane, resulting in leakage of the cytoplasmic content. They also inhibit fungal sporulation and mycelia growth. More specifically, mycotoxin and organic acid production were decreased, and the extracellular enzyme profile of *A. niger* was affected by the presence of AgNPs [65].

Regarding the synthesis conditions, the tannin concentration evaluated (500 ppm) was efficient in terms of obtaining smaller, stable NPs with higher antifungal activity. This is promising in terms of the process economy, which does not present any waste at the end of the synthesis. In this way, the NPs suspensions obtained were used as additives directly in the preparation of the sol-gel. This brings the process closer to the precepts of green synthesis [66].

3.3. Characterization of the ceramic material and the formulated coatings

The characterization of the commercial untreated ceramic material used was performed. The water absorption, relative porosity, apparent specific weight and apparent specific weight in water were determined: 29 wt%, 42%, 1.41 g/cm^3 and 0.9 g/cm^3, respectively. In addition, the porous distribution of the clay brick by MIP was determined to size larger than 7.3 nm, obtaining a frequent pore volume of 264.07 mm^3/g. In the Fig. 4A, the pore distribution reveals that the microstructure of the clay brick is predominantly comprised of pores with sizes less than 0.9 μm. In this context, Graziani *et al*. reported that the diameter of pores in highly porous specimens was over twice as large (~0.94 μm) as the diameter of pores in low-porosity specimens (~0.38 μm) [67]. Buchner et al. have shown that the high porosity in bricks (approximately 45%) can be attributed to the carbonate content (calcite and dolomite) in the raw material [21]. The porosity of clay bricks played a key role in the biodeterioration process, where lower biofilm coverage has been reported in low porous specimens [67]. In this sense, several papers

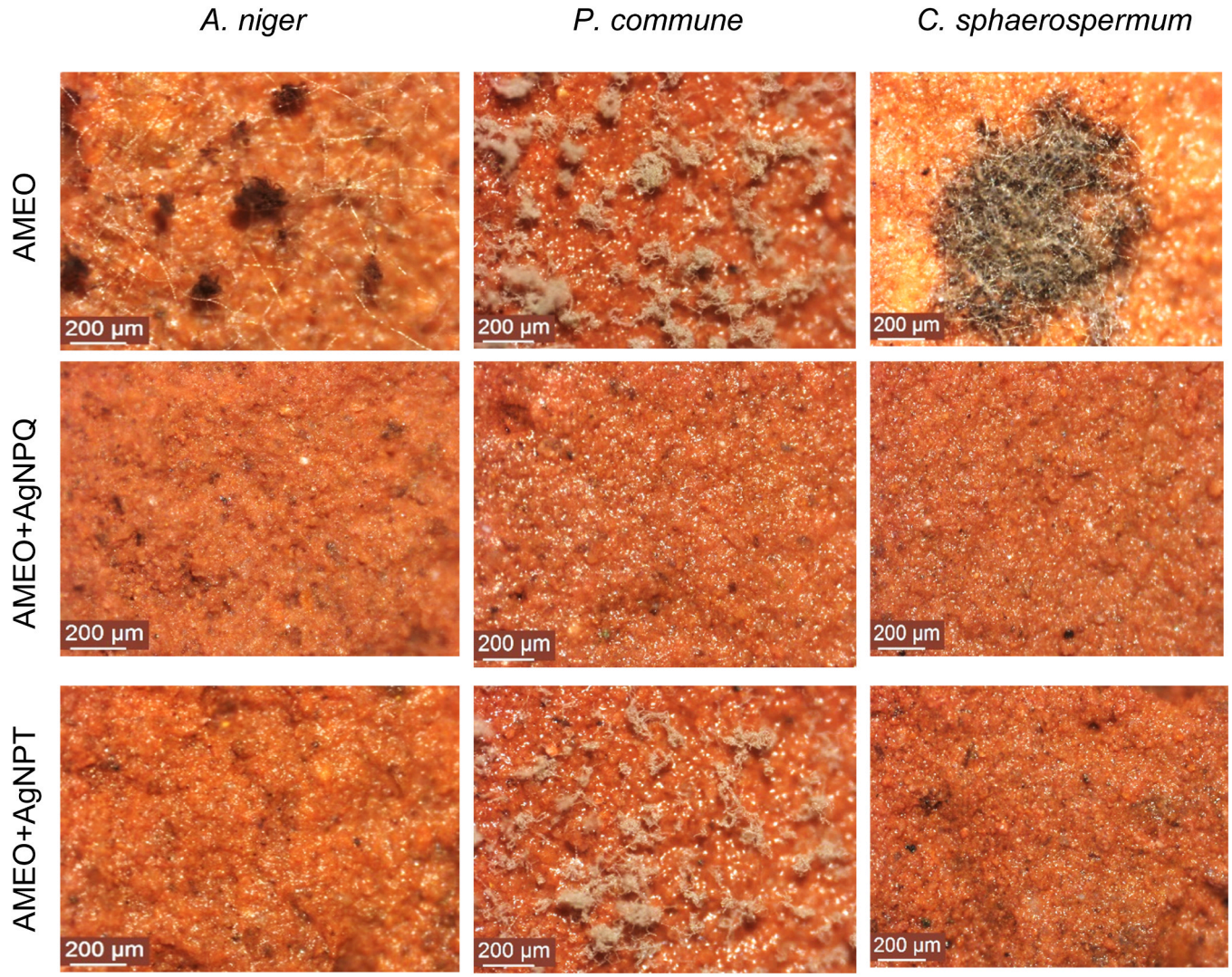

Fig. 5. Stereophotographs (80 ×) of the fungal resistance test of sol-gel coatings with AMEO, t = 30 days, T = 28 °C.

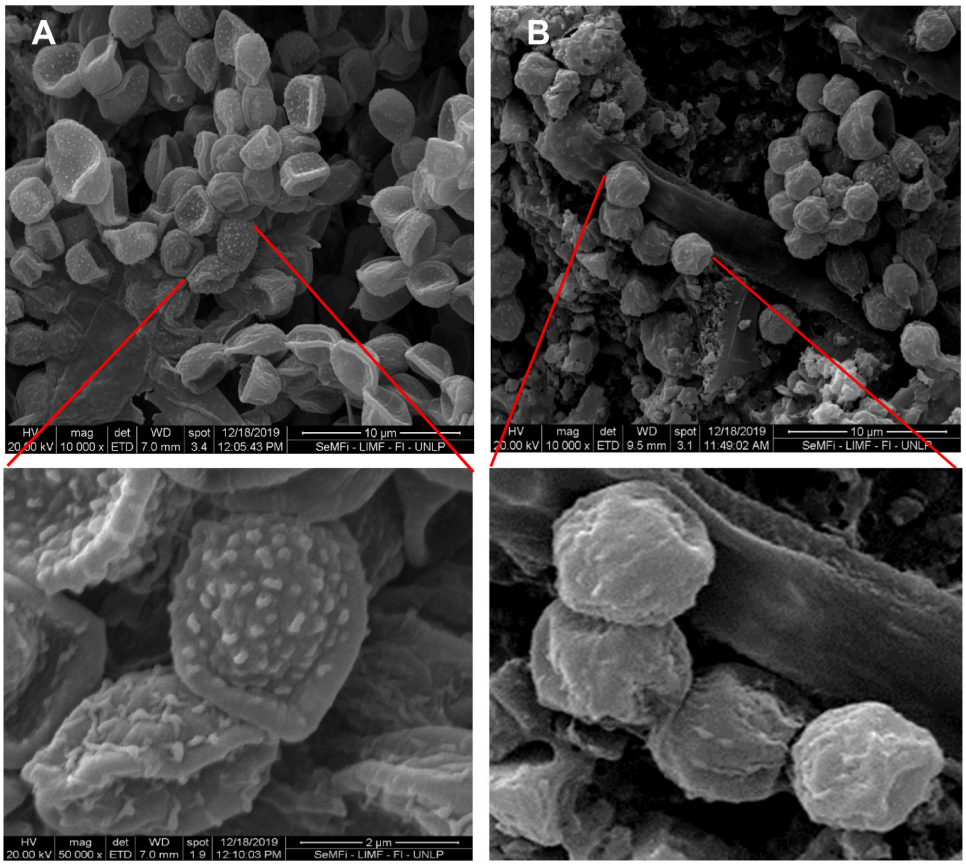

Fig. 6. SEM micrograph of *P. commune* of the fungal resistance test of sol-gel coatings. A: Without treatment (control) and B: AMEO + AgNPT. Detail of the ornamentations on the phialoconidia.

explain the influence of these parameters on the implantation of microorganisms [68,69]. For example, Graziani et al. [1] were conducted biofouling tests on fired brick substrata with different intrinsic characteristics (relative porosity) by means of an accelerated growth test.

Fig. 4 B-F shows the contact angle values for untreated (Fig. 4B) and treated bricks (Fig. 4 C, D, E and F). The contact angle of the bricks treated with silanes and nanoparticles was greater than 90°, thus providing a hydrophobic coating that offers protection against water content and the proliferation of non-xerophilic fungi (represented by *A. niger* and *P.commune*). In this sense, Grant et al. [70] carried out a study on fungi growing on structural materials and divided them into three groups according to their water requirements in laboratory substrates: primary (e.g. *Penicillium* sp. and *Aspergillus* sp.), secondary (e.g. *Cladosporium* sp. and *Alternaria* sp.) and tertiary colonisers (*Stachybotrys* sp., *Chaetomium* sp., *Trichoderma* sp. and *Auraeobasidium* sp.).

3.4. Fungal resistance test of coatings

Table 2 shows the fungal growth rating according to the area covered. The control sample inoculated with *A. niger* and *P.commune* had heavy growth, while *C. sphaerospermum* occupied 30–60% of the sample surface (moderate growth). Meanwhile, all strains showed moderate growth on the samples coated only with AMEO. On the other hand, *A. niger*, *P. commune* and *C. sphaerospermum* had heavy, moderate and light growth, respectively, when they were confronted with samples coated only with MTMO. However, in samples that were treated with silane+AgNPs, much less fungal growth was observed, showing total inhibition with AMEO+AgNPQ. Therefore, coatings with AgNPQ showed better antifungal performance than coatings functionalized with AgNPT.

Stereophotographs of the fungal resistance test of sol-gel coatings are illustrated in the Fig. 5 In the samples treated with AMEO, somatic and reproductive mycelium of the inoculated strains was observed. In the samples treated with AMEO+AgNPQ, total inhibition of microbial growth was observed, due to the absence of fungal structures. Therefore, the antifungal activity of AMEO+ Ag5NPQ and AMEO+ Ag5NPT may then be due to the presence of NPs retained in the silane matrix coupled with the effect of hydrophobic surface. However, *P. commune* was able to grow in the sample treated with AMEO+AgNPT. Fig. 6 illustrated SEM micrographs of *P. commune* of the fungal resistance test of sol-gel coatings. In the untreated sample there are numerous mutually related phialoconidia and details of the ornamentations. In the AMEO+AgNPT treated samples although there is no total growth inhibition, cell lineage with unornamented phialoconidia is prominent. Spore ornamentations have traditionally been of taxonomic importance [71,72] and *P. commune* has phialoconidial ornamentation of microverrucate or microtuberculate class. Phialoconidia without ornamentation may function as inefficient propagules in fungal dispersal, preventing the colonization of new ceramic materials and the subsequent establishment of the fungal biofilm.

Fig. 7 illustrated stereophotographs of the fungal resistance test of sol-gel coatings with MTMO, MTMO+AgNPQ and MTMO+AgNPT. Fungal growth was observed in all samples, as there is reproductive mycelium of *A. niger* and *P. commune*, while somatic mycelium of *C. sphaerospermum* is very noticeable. Evidently, there is a difference between the antifungal activity of samples treated with MTMO+AgNPs and AMEO+AgNPs, which may be related to the interactions between the amino group of AMEO with AgNPs and the mercapto group of MTMO with AgNPs. In the latter case, this interaction can lead to the formation of precipitate and the NPs may not be able to access the fungal cell system. In contrast, the association of AMEO amino groups with the AgNPs could be stronger and more stable allowing greater availability of

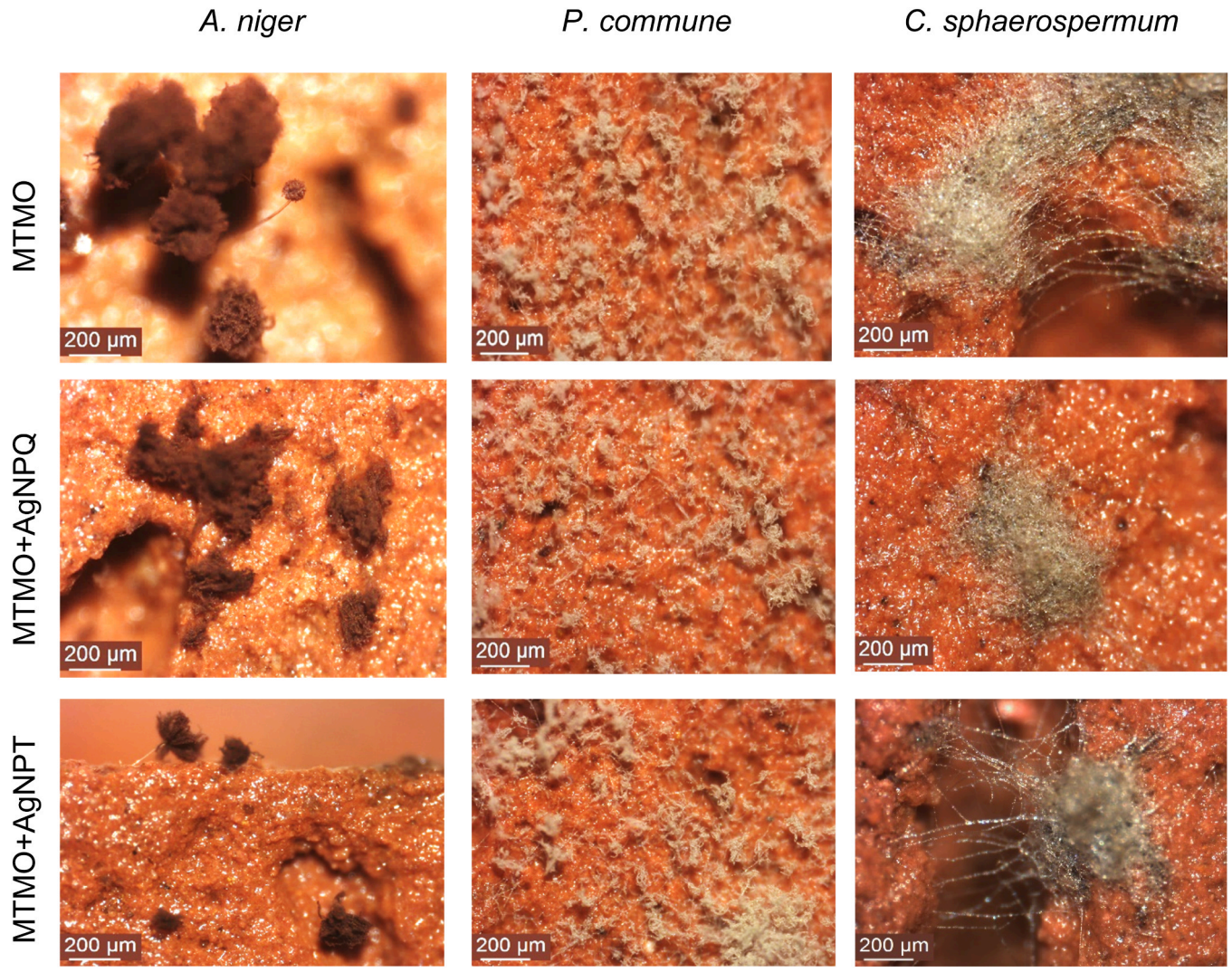

Fig. 7. Stereophotographs (80 ×) of the fungal resistance test of sol-gel coatings with MTMO, t = 30 days, T = 28 °C.

active NPs. Similar results were obtained in a study where different concentrations of the precursors (4% v/v) were used in the sol-gel coating formulation with NPs obtained from *Senna occidentalis* extract [53].

SEM images of the fungal resistance test of sol-gel coatings were depicted in Fig. 8. The fungal structures of the studied strains were absent in the samples treated with AMEO+AgNPQ. However, phialoconidia and conidiophores of *A. niger* are observed on samples treated with AMEO and MTMO, respectively. The phialoconidia of *A. niger* developed on MTMO+AgNPQ do not show any ornamentation, possibly due to the presence of AgNPQ, a phenomenon similar to that described in Fig. 6 for *P. commune*. In the samples treated with AMEO, MTMO and MTMO-+AgNPQ were observed conidia and somatic mycelium of *P.commune* and *C. sphaerospermum*, respectively.

Fig. 9 provides SEM micrograph, mapping and EDS spectra of *P. commune* on ceramic material. Fig. 9A shows abundant phialoconidia with ornamentations together with crystal structures of acicular morphology. The mapping shows the distribution of Ca, Si, Al and C over the sample (Fig. 9B) and the appearance of a strong signal corresponding to Ca confirmed in the EDS spectra of the cristal structures studied (Fig. 9 C and D). In both spectra, intense peaks of oxygen and calcium are observed at 0.5 and 3.7 keV, respectively. These results and the fact that similar morphology structures have been reported in the study on the role of fungi in calcite biomineralisation indicate that the observed formations would be calcium oxalate [73]. *Penicillium* sp. are known to produce oxalic acid or to contribute to the formation of calcium oxalate crystals. From the acidic molecules synthesized by fungi, oxalic acid may be one of the most important fungal produced acids being responsible for solubilization of metals such as iron, aluminum, lithium and manganese to form oxalates [74].

The results described are promising due to the obtaining of coating functionalized with antifungal NPs efficient in the control of ceramic materials biodeterioration. Due to abiotic (temperature and humidity) and biotic (deteriorating organisms) factors, materials tend to deteriorate over time, losing some of their original properties. Therefore, this coating can function as a protection system to extend the service life of the material. However, it is recommended to test the efficiency of this coating for more than 30 days carrying out weathering resistance tests to check its use on outdoor ceramic materials.

Considering the challenges and future prospective, this coating will be directly applied to building construction materials and its resistance to biodeterioration will be assessed *in situ*. This will enable us to test the actual durability of the coatings antifungal performance within the microbial *consortium*. Additionally, NPs can be synthesized from other metallic solutions and tannins from different South American plants, aiming to achieve antifungal activity and their incorporation into the sol-gel coatings.

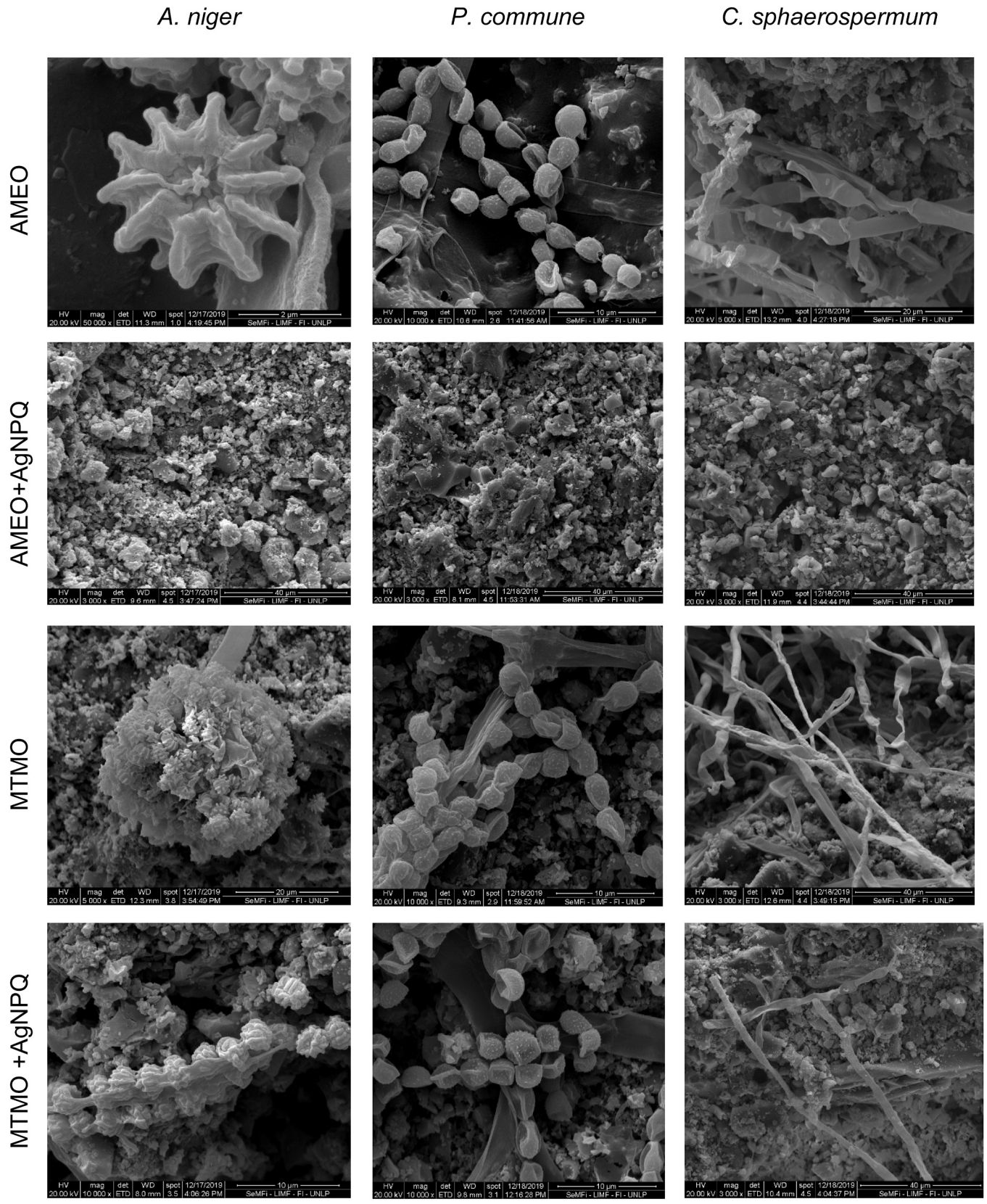

Fig. 8. SEM images of the fungal resistance test of sol-gel coatings, t = 30 days, T = 28 °C.

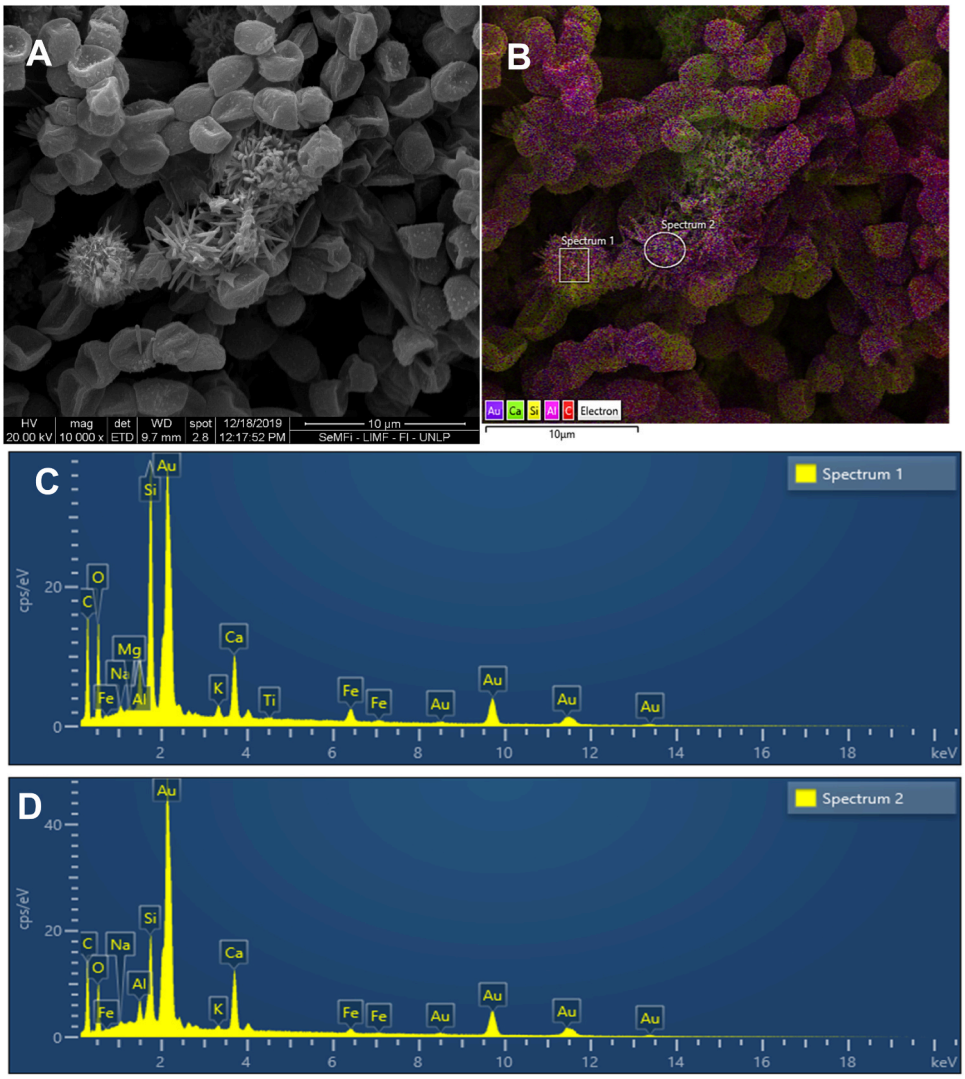

Fig. 9. *P. commune* on ceramic material. A: SEM micrograph, B: Mapping, C and D: EDS spectra, t = 30 days, T = 28 °C.

4. Conclusions

Following the precepts of green chemistry, it was possible to efficiently obtain antifungal silver nanoparticles from *Caesalpinia spinosa* and *Schinopsis balansae* tannin solution.

UV-Vis and FTIR spectroscopy, TEM and particle size determination were efficient techniques in the characterization of nanoparticles.

3-aminopropyl triethoxysilane and 3-mercaptopropyltrimethoxysilane are excellent precursors to obtain hydrophobic protective sol-gel coatings to be apply on ceramic materials and improve their resistance to fungal growth.

The silane water-alcoholic solutions can be used to functionalize silver nanoparticles efficiently.

It should be noted that the treatment of the bricks is carried out through a process without energy cost since it can be done at room temperature therefore, this type of coating could be applied under normal service conditions.

The sol- gel coatings can be characterized by contact angle measurements and bioassays to assess the ceramic fungal resistance employing *Aspergillus niger*, *Penicillium commune* and *Cladosporium sphaerospermum*. SEM and EDS were employed to study the coated surfaces, showing the different biofilms formed.

3-aminopropyl triethoxysilane and 3-mercaptopropyltrimethoxysilane additivated with silver nanoparticles can control the fungal growth on ceramic surfaces.

Sol-gel coatings from 3-aminopropyl triethoxysilane and silver nanoparticles are the better protection system for ceramic materials against degradation, and therefore improve of building biodeterioration control.

Sol-gel coatings with antimicrobial nanoparticles can be employed as a protective system for paints, in the metallurgical industry to prevent biocorrosion, in the conservation and restoration of historical heritage monuments and for the maintenance of construction materials.

CRediT authorship contribution statement

Dr. Erasmo Gámez-Espinosa: Conceptualization, Methodology, Investigation, Writing - original draft. **Dra. Cecilia Deyá:** Conceptualization, Visualization Methodology, Supervision. **Dra. Marta Cabello:** Conceptualization, Visualization, Methodology, Supervision. **Dra. Natalia Bellotti:** Conceptualization, Methodology, Resources, Visualization, Project administration; Writing - review & editing, Supervision, Funding acquisition.

Declaration of Competing Interest

The authors declare that they have no known competing financial interests or personal relationships that could have appeared to influence

the work reported in this paper.

Data availability

Data will be made available on request.

Acknowledgment

Authors are thankfull of the essential support of: Consejo Nacional de Investigaciones Científicas y Técnicas (CONICET), Argentina, Comisión de Investigaciones Científicas de la provincia de Buenos Aires (CICPBA), Argentina, Agencia Nacional de Promoción Científica y Tecnológica (ANPCyT), Argentina and Universidad Nacional de La Plata (UNLP), Argentina. They also thank the technical support of the Ing. Pablo Bellotti and Lic. Claudio Cerruti.

References

[1] L. Graziani, E. Quagliarini, M. D'Orazio, TiO2-treated different fired brick surfaces for biofouling prevention: experimental and modelling results, Ceram. Int. 42 (2016) 4002–4010, https://doi.org/10.1016/j.ceramint.2015.11.069.
[2] C. Gaylarde, M.R. Silva, T. Warscheid, Microbial impact on building materials: an overview, Mater. Struct. 36 (2003) 342–352, https://doi.org/10.1617/13867.
[3] M. Romani, T. Warscheid, L. Nicole, L. Marcon, P. Di Martino, M.T. Suzuki, P. Lebaron, R. Lami, Current and future chemical treatments to fight biodeterioration of outdoor building materials and associated biofilms: moving away from ecotoxic and towards efficient, sustainable solutions, Sci. Total Environ. 802 (2022), 149846, https://doi.org/10.1016/j.scitotenv.2021.149846.
[4] D. Allsopp, Worldwide wastage: the economics of biodeterioration, Q. Mag. Soc. Gen. Microbiol. 38 (2011) 150–153.
[5] V. Ivanov, V. Stabnikov, Introduction to viruses, bacteria, and fungi in the built environment, in: Viruses, Bact. Fungi Built Environ., Elsevier, 2022, pp. 11–27, https://doi.org/10.1016/B978-0-323-85206-7.00004-6.
[6] E. Gámez-Espinosa, Estudio de la micobiota presente en materiales estructurales: relación con su deterioro y control mediante recubrimientos de base sol-gel con nanopartículas obtenidas por síntesis verde. Tesis presentada para optar por el grado de Doctor., Universidad Nacional de La Plata, 2022. doi:10.35537/10915/135399.
[7] D.S. Paiva, L. Fernandes, J. Trovão, N. Mesquita, I. Tiago, A. Portugal, Uncovering the fungal diversity colonizing limestone walls of a forgotten monument in the central region of portugal by high-throughput sequencing and culture-based methods, Appl. Sci. 12 (2022) 10650, https://doi.org/10.3390/app122010650.
[8] E.B.G. Jones, Fungal adhesion, Mycol. Res. 98 (1994) 961–981, https://doi.org/10.1016/S0953-7562(09)80421-8.
[9] B.E. Priegnitz, A. Wargenau, U. Brandt, M. Rohde, S. Dietrich, A. Kwade, R. Krull, A. Fleißner, The role of initial spore adhesion in pellet and biofilm formation in Aspergillus niger, Fungal Genet. Biol. 49 (2012) 30–38, https://doi.org/10.1016/j.fgb.2011.12.002.
[10] M.W. Harding, L.L.R. Marques, R.J. Howard, M.E. Olson, Can filamentous fungi form biofilms? Trends Microbiol 17 (2009) 475–480, https://doi.org/10.1016/j.tim.2009.08.007.
[11] P. Berdahl, H. Akbari, R. Levinson, W.A. Miller, Weathering of roofing materials – an overview, Constr. Build. Mater. 22 (2008) 423–433, https://doi.org/10.1016/j.conbuildmat.2006.10.015.
[12] M.L. Coutinho, A.Z. Miller, M.F. Macedo, Biological colonization and biodeterioration of architectural ceramic materials: an overview, J. Cult. Herit. 16 (2015) 759–777, https://doi.org/10.1016/j.culher.2015.01.006.
[13] P.D. Martino, What about biofilms on the surface of stone monuments? Open Conf. Proc. J. 6 (2016) 14–28, https://doi.org/10.2174/2210289201607020014.
[14] R.J.B. Cordero, A. Casadevall, Functions of fungal melanin beyond virulence, Fungal Biol. Rev. 31 (2017) 99–112, https://doi.org/10.1016/j.fbr.2016.12.003.
[15] R.I. Adams, S. Bhangar, K.C. Dannemiller, J.A. Eisen, N. Fierer, J.A. Gilbert, J. L. Green, L.C. Marr, S.L. Miller, J.A. Siegel, B. Stephens, M.S. Waring, K. Bibby, Ten questions concerning the microbiomes of buildings, Build. Environ. 109 (2016) 224–234, https://doi.org/10.1016/j.buildenv.2016.09.001.
[16] J. Pena-Poza, C. Ascaso, M. Sanz, S. Pérez-Ortega, M. Oujja, J. Wierzchos, V. Souza-Egipsy, M.V. Cañamares, M. Urizal, M. Castillejo, M. García-Heras, Effect of biological colonization on ceramic roofing tiles by lichens and a combined laser and biocide procedure for its removal, Int. Biodeterior. Biodegrad. 126 (2018) 86–94, https://doi.org/10.1016/j.ibiod.2017.10.003.
[17] L. Graziani, M. D'Orazio, Biofouling prevention of ancient brick surfaces by TiO2-based nano-coatings, Coatings 5 (2015) 357–365, https://doi.org/10.3390/coatings5030357.
[18] K. Ramakrishnan, V. Chellappa, S. Chandrasekarabarathi, Manufacturing of low-cost bricks using waste materials, Mater. Proc. 13 (2023), https://doi.org/10.3390/materproc2023013025.
[19] S. Lawanwadeekul, A. Srisuwan, N. Phonphuak, P. Chindaprasirt, Enhancement of porosity and strength of clay brick fired at reduced temperature with the aid of corn cob and waste glass, Constr. Build. Mater. 369 (2023), 130547, https://doi.org/10.1016/j.conbuildmat.2023.130547.
[20] Z. Moujoud, A. Harrati, A. Manni, A. Naim, A. El Bouari, O. Tanane, Study of fired clay bricks with coconut shell waste as a renewable pore-forming agent: technological, mechanical, and thermal properties, J. Build. Eng. 68 (2023), 106107, https://doi.org/10.1016/j.jobe.2023.106107.
[21] T. Buchner, T. Kiefer, L. Zelaya-Lainez, W. Gaggl, T. Konegger, J. Füssl, A multitechnique, quantitative characterization of the pore space of fired bricks made of five clayey raw materials used in European brick industry, Appl. Clay Sci. 200 (2021), 105884, https://doi.org/10.1016/j.clay.2020.105884.
[22] R. Arreche, K. Igal, N. Bellotti, P. Vázquez, Microbiological prevention using functionalized materials as ecological additives in hygienic paints, Procedia Mater. Sci. 9 (2015) 635–642, https://doi.org/10.1016/j.mspro.2015.05.040.
[23] M.A. Fernández, L. Barberia Roque, E. Gámez Espinosa, C. Deyá, N. Bellotti, Organo-montmorillonite with biogenic compounds to be applied in antifungal coatings, Appl. Clay Sci. 184 (2020), https://doi.org/10.1016/j.clay.2019.105369.
[24] L.L. Hench, J.K. West, The sol-gel process, Chem. Rev. 90 (1990) 33–72, https://doi.org/10.1021/cr00099a003.
[25] S. Sakka, Birth of the sol–gel method: early history, J. Sol. -Gel Sci. Technol. (2021), https://doi.org/10.1007/s10971-021-05640-9.
[26] R. Gupta, A. Kumar, Bioactive materials for biomedical applications using sol–gel technology, Biomed. Mater. 3 (2008), 034005, https://doi.org/10.1088/1748-6041/3/3/034005.
[27] J. Wen, G.L. Wilkes, Organic/Inorganic hybrid network materials by the sol−gel approach, Chem. Mater. 8 (1996) 1667–1681, https://doi.org/10.1021/cm9601143.
[28] C. Ohtsuki, T. Miyazaki, M. Tanihara, Development of bioactive organic–inorganic hybrid for bone substitutes, Mater. Sci. Eng. C. 22 (2002) 27–34, https://doi.org/10.1016/S0928-4931(02)00109-1.
[29] C.J. Brinker, G.W. Scherer, Aging of gels, in: Sol-Gel Sci. Phys. Chem. Sol–Gel Process., Elsevier, 1990, pp. 356–405, https://doi.org/10.1016/B978-0-08-057103-4.50011-8.
[30] L.B. Capeletti, M. do Carmo Martins Alves, M.B. Cardoso, J.H.Z. dos Santos, Hybrid silica based catalysts prepared by the encapsulation of zirconocene compound via non-hydrolytic sol-gel method for ethylene polymerization, Appl. Catal. A Gen. 560 (2018) 225–235, https://doi.org/10.1016/j.apcata.2018.03.013.
[31] X. Wang, H.C. Schröder, U. Schloßmacher, L. Jiang, M. Korzhev, W.E.G. Müller, Biosilica aging: from enzyme-driven gelation via syneresis to chemical/biochemical hardening, Biochim. Biophys. Acta - Gen. Subj. 1830 (2013) 3437–3446, https://doi.org/10.1016/j.bbagen.2013.02.006.
[32] C.J. Brinker, G.W. Scherer, Film formation, in: Sol-Gel Sci. Phys. Chem. Sol–Gel Process., Elsevier, United States of America, 1990, pp. 786–837, https://doi.org/10.1016/B978-0-08-057103-4.50018-0.
[33] C.M. Halliwell, A.E.G. Cass, A factorial analysis of silanization conditions for the immobilization of oligonucleotides on glass surfaces, Anal. Chem. 73 (2001) 2476–2483, https://doi.org/10.1021/ac0010633.
[34] A. Zanurin, N.A. Johari, J. Alias, H. Mas Ayu, N. Redzuan, S. Izman, Research progress of sol-gel ceramic coating: a review, Mater. Today Proc. (2021), https://doi.org/10.1016/j.matpr.2021.09.203.
[35] G.J. Copello, S. Teves, J. Degrossi, M. D'Aquino, M.F. Desimone, L.E. Díaz, Proving the antimicrobial spectrum of an amphoteric surfactant-sol-gel coating: a food-borne pathogen study, J. Ind. Microbiol. Biotechnol. 35 (2008) 1041–1046, https://doi.org/10.1007/s10295-008-0380-3.
[36] A. Presentato, F. Armetta, A. Spinella, D.F. Chillura Martino, R. Alduina, M. L. Saladino, Formulation of mesoporous silica nanoparticles for controlled release of antimicrobials for stone preventive conservation, Front. Chem. 8 (2020), https://doi.org/10.3389/fchem.2020.00699.
[37] V. Purcar, V. Rădiţoiu, F.M. Raduly, A. Rădiţoiu, M. Anastasescu, M. Popa, S. Căprărescu, R. Şomoghi, M. Constantin, C. Firincă, G.C. Ispas, Physicochemical and morphological properties of hybrid films containing silver-based silica materials deposited on glass substrates, Coatings 12 (2022) 242, https://doi.org/10.3390/coatings12020242.
[38] D. Mosselhy, Y. Ge, M. Gasik, K. Nordström, O. Natri, S.-P. Hannula, Silica-gentamicin nanohybrids: synthesis and antimicrobial action, Mater. (Basel) 9 (2016) 170, https://doi.org/10.3390/ma9030170.
[39] V. Purcar, V. Rădiţoiu, C. Nichita, A. Bălan, A. Rădiţoiu, S. Căprărescu, F. M. Raduly, R. Manea, R. Şomoghi, C.-A. Nicolae, I. Raut, L. Jecu, Preparation and characterization of silica nanoparticles and of silica-gentamicin nanostructured solution obtained by microwave-assisted synthesis, Mater. (Basel) 14 (2021) 2086, https://doi.org/10.3390/ma14082086.
[40] E. Gámez-Espinosa, C. Deyá, F. Ruiz, N. Bellotti, LONG-TERM field study of a Waterborne paint with a nano-additive for biodeterioration control, J. Build. Eng. 50 (2022), 104148, https://doi.org/10.1016/j.jobe.2022.104148.
[41] E. Gámez-Espinosa, L. Barberia-Roque, N. Bellotti, Role of nanotechnology in the management of indoor fungi, in: Nanobiotechnology Diagnosis, Drug Deliv. Treat., First, Wiley, 2020, pp. 229–257, https://doi.org/10.1002/9781119671732.ch12.
[42] M.K. Al-Sakkaf, S.A. Onaizi, Rheology, characteristics, stability, and pH-responsiveness of biosurfactant-stabilized crude oil/water nanoemulsions, Fuel 307 (2022), 121845, https://doi.org/10.1016/j.fuel.2021.121845.
[43] P. Ganguli, S. Chaudhuri, Nanomaterials in antimicrobial paints and coatings to prevent biodegradation of man-made surfaces: a review, Mater. Today Proc. 45 (2021) 3769–3777, https://doi.org/10.1016/j.matpr.2021.01.275.
[44] D. Liu, L. Li, T. You, Superior catalytic performances of platinum nanoparticles loaded nitrogen-doped graphene toward methanol oxidation and hydrogen evolution reaction, J. Colloid Interface Sci. 487 (2017) 330–335, https://doi.org/10.1016/j.jcis.2016.10.038.
[45] C. Huo, M. Khoshnamvand, P. Liu, C.-G. Yuan, W. Cao, Eco-friendly approach for biosynthesis of silver nanoparticles using Citrus maxima peel extract and their

characterization, catalytic, antioxidant and antimicrobial characteristics, Mater. Res. Express 6 (2018), 015010, https://doi.org/10.1088/2053-1591/aae34c.
[46] G.A. Naikoo, M. Mustaqeem, I.U. Hassan, T. Awan, F. Arshad, H. Salim, A. Qurashi, Bioinspired and green synthesis of nanoparticles from plant extracts with antiviral and antimicrobial properties: a critical review, J. Saudi Chem. Soc. 25 (2021), 101304, https://doi.org/10.1016/j.jscs.2021.101304.
[47] P. Mohammadi, A. Abdi Ali, P. Ghadam, Mycogenic nanoparticles and their applications as antimicrobial and antibiofilm agents in postharvest stage, in: Fungal Cell Factories Sustain. Nanomater. Prod. Agric. Appl., Elsevier, 2023, pp. 635–655, https://doi.org/10.1016/B978-0-323-99922-9.00021-0.
[48] T. Jasrotia, S. Chaudhary, A. Kaushik, R. Kumar, G.R. Chaudhary, Green chemistry-assisted synthesis of biocompatible Ag, Cu, and Fe2O3 nanoparticles, Mater. Today Chem. 15 (2020), 100214, https://doi.org/10.1016/j.mtchem.2019.100214.
[49] I. Corsi, M. Winther-Nielsen, R. Sethi, C. Punta, C. Della Torre, G. Libralato, G. Lofrano, L. Sabatini, M. Aiello, L. Fiordi, F. Cinuzzi, A. Caneschi, D. Pellegrini, I. Buttino, Ecofriendly nanotechnologies and nanomaterials for environmental applications: Key issue and consensus recommendations for sustainable and ecosafe nanoremediation, Ecotoxicol. Environ. Saf. 154 (2018) 237–244, https://doi.org/10.1016/j.ecoenv.2018.02.037.
[50] Bellotti, B. del Amo, R. Romagnoli, Quaternary ammonium “tannate” for antifouling coatings, Ind. Eng. Chem. Res. 51 (2012) 16626–16632, https://doi.org/10.1021/ie301524r.
[51] C. Deyá, N. Bellotti, Biosynthesized silver nanoparticles to control fungal infections in indoor environments, Adv. Nat. Sci. Nanosci. Nanotechnol. 8 (2017), 025005, https://doi.org/10.1088/2043-6254/aa6880.
[52] E. Gámez-Espinosa, N. Bellotti, C. Deyá, M. Cabello, Mycological studies as a tool to improve the control of building materials biodeterioration, J. Build. Eng. 32 (2020), 101738, https://doi.org/10.1016/j.jobe.2020.101738.
[53] E. Gámez-Espinosa, L. Barberia-Roque, O.F. Obidi, C. Deyá, N. Bellotti, Antifungal applications for nano-additives synthesized with a bio-based approach, Adv. Nat. Sci. Nanosci. Nanotechnol. 11 (2020), 015019, https://doi.org/10.1088/2043-6254/ab790f.
[54] K. Koch, W. Barthlott, Superhydrophobic and superhydrophilic plant surfaces: an inspiration for biomimetic materials, Philos. Trans. R. Soc. A Math. Phys. Eng. Sci. 367 (2009) 1487–1509, https://doi.org/10.1098/rsta.2009.0022.
[55] ASTM D5590, Standard Test Method for Determining the Resistance of Paint films and Related Coatings to Fungal Defacement by Accelerated Four-Week Agar Plate Assay, ASTM International, West Conshohocken, PA, 2010.
[56] M.F. Simões, C. Santos, N. Lima, Structural diversity of aspergillus (section nigri) spores, Microsc. Microanal. 19 (2013) 1151–1158, https://doi.org/10.1017/S1431927613001712.
[57] M.M. Abdo, M.I. Abdel-Hamid, I.M. El-Sherbiny, G. El-Sherbeny, E.I. Abdel-Aal, Green synthesis of AgNPs, alginate microbeads and Chlorella minutissima laden alginate microbeads for tertiary treatment of municipal wastewater, Bioresour. Technol. Rep. 21 (2023), 101300, https://doi.org/10.1016/j.biteb.2022.101300.
[58] M. Shateri Khalil-Abad, M.E. Yazdanshenas, M.R. Nateghi, Effect of cationization on adsorption of silver nanoparticles on cotton surfaces and its antibacterial activity, Cellulose 16 (2009) 1147–1157, https://doi.org/10.1007/s10570-009-9351-8.
[59] K.S. Singh, M.S. Majik, S. Tilvi, Vibrational spectroscopy for structural characterization of bioactive compounds, in: Anal. Mar. Samples Search Bioact. Compd., Elsevier B.V, 2014, pp. 115–148, https://doi.org/10.1016/B978-0-444-63359-0.00006-9.
[60] R. Morrison, R. Boyd, Organic Chemistry, Fifth, Allyn & Bacon, Boston, Massachusetts, United States, 1990.
[61] C.V. Restrepo, C.C. Villa, Synthesis of silver nanoparticles, influence of capping agents, and dependence on size and shape: A review, Environ. Nanotechnol., Monit. Manag. 15 (2021), 100428, https://doi.org/10.1016/j.enmm.2021.100428.
[62] S. Chen, J.R. Drehmel, R.L. Penn, Facile synthesis of monodispersed Ag NPs in ethylene glycol using mixed capping agents, ACS Omega 5 (2020) 6069–6073, https://doi.org/10.1021/acsomega.9b04492.
[63] J. Guo, H. Wu, X. Liao, B. Shi, Facile synthesis of size-controlled silver nanoparticles using plant tannin grafted collagen fiber as reductant and stabilizer for microwave absorption application in the whole Ku band, J. Phys. Chem. C 115 (2011) 23688–23694, https://doi.org/10.1021/jp207194a.
[64] G. Rajkumar, R. Sundar, Biogenic one-step synthesis of silver nanoparticles (AgNPs) using an aqueous extract of Persea americana seed: characterization, phytochemical screening, antibacterial, antifungal and antioxidant activities, Inorg. Chem. Commun. 143 (2022), 109817, https://doi.org/10.1016/j.inoche.2022.109817.
[65] K. Pietrzak, M. Twarużek, A. Czyżowska, R. Kosicki, B. Gutarowska, Influence of silver nanoparticles on metabolism and toxicity of moulds, Acta Biochim. Pol. 62 (2015) 851–857, https://doi.org/10.18388/abp.2015_1146.
[66] V.G. Zuin, Circularity in green chemical products, processes and services: innovative routes based on integrated eco-design and solution systems, Curr. Opin. Green. Sustain. Chem. 2 (2016) 40–44, https://doi.org/10.1016/j.cogsc.2016.09.008.
[67] L. Graziani, E. Quagliarini, A. Osimani, L. Aquilanti, F. Clementi, M. D'Orazio, The influence of clay brick substratum on the inhibitory efficiency of T i O 2 nanocoating against biofouling, Build. Environ. 82 (2014) 128–134, https://doi.org/10.1016/j.buildenv.2014.08.013.
[68] L. Graziani, M. D'Orazio, Biofouling prevention of ancient brick surfaces by TiO2-based nano-coatings, Coatings 5 (2015) 357–365, https://doi.org/10.3390/coatings5030357.
[69] L. Graziani, E. Quagliarini, M. D'Orazio, TiO2-treated different fired brick surfaces for biofouling prevention: experimental and modelling results, Ceram. Int. 42 (2016) 4002–4010, https://doi.org/10.1016/j.ceramint.2015.11.069.
[70] C. Grant, C.A. Hunter, B. Flannigan, A.F. Bravery, The moisture requirements of moulds isolated from domestic dwellings, Int. Biodeterior. 25 (1989) 259–284, https://doi.org/10.1016/0265-3036(89)90002-X.
[71] Z. Kozakiewicz, Ornamentation types of conidia and conidiogenous structures in fasciculate Penicillium species using scanning electron microscopy, Bot. J. Linn. Soc. 99 (1989) 273–293, https://doi.org/10.1111/j.1095-8339.1989.tb00404.x.
[72] J. Houbraken, S. Kocsubé, C.M. Visagie, N. Yilmaz, X.-C. Wang, M. Meijer, B. Kraak, V. Hubka, K. Bensch, R.A. Samson, J.C. Frisvad, Classification of Aspergillus, Penicillium, Talaromyces and related genera (Eurotiales): an overview of families, genera, subgenera, sections, series and species, Stud. Mycol. 95 (2020) 5–169, https://doi.org/10.1016/j.simyco.2020.05.002.
[73] S. Bindschedler, G. Cailleau, E. Verrecchia, Role of fungi in the biomineralization of calcite, Minerals 6 (2016) 41, https://doi.org/10.3390/min6020041.
[74] G.M. Gadd, J. Bahri-Esfahani, Q. Li, Y.J. Rhee, Z. Wei, M. Fomina, X. Liang, Oxalate production by fungi: significance in geomycology, biodeterioration and bioremediation, Fungal Biol. Rev. 28 (2014) 36–55, https://doi.org/10.1016/j.fbr.2014.05.001.